

This is the accepted manuscript made available via CHORUS. The article has been published as:

Photoexcitation Dynamics in Films of C₆₀ and Zn Phthalocyanine with a Layered Nanostructure

Paul A. Lane, Paul D. Cunningham, Joseph S. Melinger, Gary P. Kushto, Okan Esenturk,
and Edwin J. Heilweil

Phys. Rev. Lett. **108**, 077402 — Published 15 February 2012

DOI: [10.1103/PhysRevLett.108.077402](https://doi.org/10.1103/PhysRevLett.108.077402)

Photoexcitation Dynamics in Nanolayered Films of C₆₀ and Zinc Phthalocyanine

Paul A. Lane, Paul D. Cunningham, Joseph S. Melinger, and Gary P. Kushto
U.S. Naval Research Laboratory, 4555 Overlook Ave. SW, Washington, DC 20375

Okan Esenturk* and Edwin J. Heilweil
National Institute of Standards and Technology, Gaithersburg, MD 20899*

We elucidate photoexcitation dynamics in C₆₀ and zinc phthalocyanine (ZnPc) from ps to ms by transient absorption and time-resolved THz spectroscopy. Autoionization of C₆₀ creates a charge transfer state that is a precursor to photocarrier generation. Decay of the THz signal is due to decreasing photocarrier mobility over the first 20 ps and thereafter reflects recombination dynamics. Singlet diffusion rates in C₆₀ are determined by modeling the rise of ground state bleaching of ZnPc absorption following C₆₀ excitation. Recombination dynamics transform from bimolecular to monomolecular as the layer thickness is reduced, revealing a metastable exciplex at the C₆₀/ZnPc interface with a lifetime of 150 μ s.

Organic solar cell¹ performance has dramatically improved over the past decade due to materials advances and optimization of film morphology.^{2,3} Solution-processed blends self-organize into segregated domains,⁴ whereas co-sublimed blends have an amorphous structure that impedes transport.⁵ Recent advances in sublimed cells³ have renewed interest in charge generation in molecular systems with particular attention on charge transfer between C₆₀ and phthalocyanines.^{6,7} The C₆₀/phthalocyanine heterojunction is an archetype for sublimed cells, yet there are relatively few studies of excited state dynamics in this system.^{8–10} A better understanding of excitation dynamics in this model system has broad implications.

In this Letter we elucidate charge transfer and photoexcitation dynamics in C₆₀ and zinc phthalocyanine (ZnPc) films. Time-resolved THz spectroscopy (TRTS) is a powerful, non-contact probe of photoconductivity,¹¹ yet its application to organic semiconductors is controversial. Interpretation of the frequency-dependent complex conductivity, $\sigma(\omega)$, is not straightforward as similar features over the typical THz bandwidth can be described by different models.^{12–14} Based on the shape of $\sigma(\omega)$, the sub-ps rise and decay of THz absorption has been attributed to free carriers.^{12,15} However, the addition of a fullerene acceptor to polythiophene does not enhance the initial signal^{14,16,17} nor does the addition of ZnPc to C₆₀.¹⁸ Both carrier populations and mobilities vary on a ps time scale, complicating interpretation of the temporal dependence of the conductivity.¹⁹ Transient absorption (TA) spectroscopy has been widely used to investigate photoexcitation dynamics in organic semiconductors, yet there have been no detailed comparisons of TA and THz spectroscopy in organic semiconductors. The combination of these two techniques permits us to decouple carrier mobility and populations, providing unique insight. We extend the scope of this study with continuous wave (CW) spectroscopy to identify the excited absorption bands of long-lived carriers and measure their recombination dynamics.

ZnPc and C₆₀ were purified by consecutive vacuum

train sublimation. Films were deposited onto fused silica substrates at a rate of 0.5 Å/sec in vacuum (10^{-7} Torr). Deposition rates and layer thicknesses were measured *in situ* by a calibrated quartz crystal monitor. 300 nm thick superlattice films with layers from 1 nm to 10 nm thick were prepared by alternate deposition of ZnPc and C₆₀. Neat films of ZnPc and C₆₀ and a 1:1 blend by weight of C₆₀ and ZnPc were also prepared. For TRTS, thin films were excited with a frequency-doubled Ti:Sapphire laser (60 fs, 3.1 eV, 5×10^{13} photons/pulse) and interrogated with synchronized THz probe pulses.²⁰ Optical transients were measured using an amplified fs laser system (150 fs, 3.2 eV, 10^{13} photons/pulse) as the pump and a frequency doubled optical parametric amplifier to generate the probe. Photoinduced absorption (PA) was performed using a CW argon ion laser as the pump (488 nm) and a quartz halogen lamp dispersed through a monochromator as the probe. PA spectra and transients were measured by a lock-in amplifier and a digital storage oscilloscope, respectively. The system resolution was 10 μ s. Samples were measured in ambient conditions, though dry air was used for TRTS measurements. We also tested encapsulated samples and found no significant differences in spectra and dynamics.

Fig. 1(a) shows the differential THz transmission for neat films of C₆₀ and ZnPc. The THz dynamics of the C₆₀ film consist of an instrument limited rise and exponential decay ($\tau = 0.5$ ps) with a slowly decaying residual absorption. No sharp THz transient was observed from a neat film of ZnPc nor from C₆₀ in solution or matrix isolated in polystyrene. The THz transients of C₆₀/ZnPc layered films, shown in Fig. 1(b), resemble the C₆₀ transient for early times, but the initial decay is slower. The decay of THz absorption slows within 10 ps for samples with ≥ 5 nm thick layers and continues over the first 20 ps for samples with thinner layers. The strongest signal at longer delays was observed from the 2 nm or 5 nm layered films. The signal persists past the maximum delay (600 ps) for all layered samples. The slower decay and long-lived THz absorption in blends¹⁰ and layered films²⁰ is indicative of photocarrier generation.

FIG. 1. (a) TRTS of C₆₀ (filled circles) and ZnPc (open circles) films and TA at 2.25 eV of a C₆₀ film (line). Inset: a schematic representation of the autoionization process. (b) TRTS of C₆₀/ZnPc films with 1 (black line), 2 (blue diamonds), 5 (green pluses), and 10 (red circles) nm thick layers.

FIG. 2. (a) TA ($h\nu = 2.25$ eV) and (b) GSB ($h\nu = 1.84$ eV) of layered C₆₀/ZnPc films. Solid lines show (a) a fit to bi-exponential decay and (b) a Monte Carlo simulation of GSB dynamics (see text for details).

Comparison of TRTS with transient absorption (TA) allows us to disentangle the contributions of carrier mobility and population to THz absorption. Fig. 2 shows (a) TA with the probe set to the maxima of excited state absorption by ZnPc cations ($h\nu = 2.25$ eV) and (b) the minima of ground state bleaching (GSB) of the ZnPc Q-band ($h\nu = 1.84$ eV). These energies are taken from the PA spectra (see Fig. 3). The TA dynamics contain a weak, short-lived transient followed by exponential decay with a lifetime independent of layer thickness ($\tau = 31$ ps). At later times, the TA signal decay slows, decreasing by half between 100 ps and 600 ps. The early dynamics of GSB are qualitatively different. A sub-ps TA signal arising from C₆₀ is followed by a rise in GSB of ZnPc ($\Delta T > 0$). The most significant difference in TA and GSB dynamics is that the rise in GSB is gradual and the rise time increases with layer thickness. The rise of GSB in a neat ZnPc film is instrument limited. We show below that the GSB dynamics for all layered samples originate from singlet exciton diffusion within C₆₀ layers.

We first consider the initial TRTS and TA dynamics of C₆₀ and layered films. The rise time of a neat C₆₀ film is instrument limited and is followed by sub-ps decay ($\tau = 0.5$ ps). The initial transient cannot originate from an intramolecular excited state of C₆₀ as it is not seen in solution nor in matrix isolated films. Free carriers are precluded, as the spike in THz absorption is lower in mixed films than in neat C₆₀ films.¹⁸ Furthermore, the decay time is inconsistent with long-lived photocarriers seen in mixed films of C₆₀ and ZnPc.¹⁰ Intrinsic photoconductivity in an organic solid originates from autoionization, a process in which excitation to an upper lying Franck-Condon state (S_n) is followed by charge transfer to a neighboring molecule.²¹ The geminate pair recombines or the ionized electron can escape the Coulomb potential via a thermally-activated process, subsequently generating free carriers. This process accounts for both the instrument limited rise and sub-ps decay of THz absorption. Similar TRTS transients observed in other organic semiconductors should be reconsidered in light of these results.

The observation of autoionization and recombination

in real time allows us to correlate the photocarrier yield (ϕ) with the mobility (μ) of the transferred charge:²²

$$\phi^{-1} \cong 1 + \frac{R^3}{D\tau r_c} [\exp(r_c/R) - 1] \quad (1)$$

where R is the initial pair separation, D is the diffusivity, τ is the lifetime of the geminate pair (0.5 ps), and r_c is the interaction radius (14.4 nm at 300 K for C₆₀).¹⁰ Lee *et al.* combined transient absorption and photoconductivity to determine the mobility-yield product, $\mu\phi \cong 0.025$ cm²/V sec for excitation at 2.9 eV.²⁵ Using this value and for nearest neighbors ($R = 1.0$ nm), we obtain $D = 1.25$ cm²/sec. The corresponding mobility ($D = \mu e/k_B T$) is 50 cm²/V sec, more than an order of magnitude larger than the steady state photocarrier mobility in C₆₀ (ca. 1 cm²/V sec).^{23,24}

Following initial charge transfer, the TRTS signal of all samples decays significantly over the first 20 ps. The TRTS signal decays by 40 % for samples with 5 nm and 10 nm thick layers, increasing to 50 % for 2 nm layers and 60 % for 1 nm layers. The rapid initial decay of the TRTS signal stands in stark contrast to the GSB, which is flat or rising, demonstrating that the decay of TRTS is not due to recombination. The short time TRTS dynamics thus reflect a decrease in mobility with time as photocarriers migrate to lower energy sites.²⁸ The slower decay of the THz signal of the thicker samples may be a consequence of charge transfer following singlet exciton migration within the C₆₀ layer. The TA (Fig. 2) and TRTS²⁰ signals are correlated with one another for $t > 20$ ps, reflecting recombination dynamics rather than changes in mobility. This is consistent with a recent study that compared the TA and time-resolved microwave conductivity of polymer:fullerene blends.²⁶

The slower rise of GSB of ZnPc than of TA is a consequence of singlet exciton diffusion within C₆₀ layers. Despite the fundamental role that C₆₀ plays in sublimed organic solar cells, singlet exciton diffusion in C₆₀ has not been studied directly. The extinction coefficient of C₆₀ is twice that of ZnPc at 388 nm and thus most GSB is a consequence of charge transfer following migration to an interface rather than direct excitation of ZnPc. The GSB dynamics were modeled by a Monte Carlo simulation of hopping between neighboring C₆₀ molecules followed by charge transfer with unit quantum yield at the C₆₀/ZnPc interface.²⁷ The short-lived TA of C₆₀ is also incorporated. The solid lines in the left-hand side of Fig. 2(b) show the results of the model for a hopping rate of 2.5 THz in C₆₀ and a recovery time of 90 ps in ZnPc. Rate constants ≤ 2 THz or ≥ 3 THz yielded a poor fit to the experimental data. The only parameter varied is the layer thickness, which was fixed to the measured values for the thicker films (5 nm and 10 nm). The GSB rise dynamics of the 1 nm and 2 nm layered films reveal a degree of phase segregation. The GSB peak occurs ca. 5 ps after excitation, whereas charge transfer would be sub-ps for uniformly deposited layers. Hong *et al.* found

FIG. 3. (a) PA (line) and absorption (symbols) spectra of a film with 10 nm layers. Left inset: power dependence of C_2 (squares) and GSB (circles) for samples with 2 nm (filled symbols) and 10 nm (open symbols) thick layers. Right inset: schematic diagram of orbitals and transitions of C_{60}^- and $ZnPc^+$. (b) PA (line) and absorption (symbols) spectra of a films with 2 nm layers and the PA spectrum of a $C_{60}:ZnPc$ blend (dashed line). Inset: decay of C_2 for samples with 2 nm (top trace) and 10 nm (bottom trace) thick layers.

that a similar layered film of C_{60} and $ZnPc$ has a highly crystalline structure, much more so than a blend.^{5,10} We obtained a good model of the GSB of the thinner layered samples by introducing rough domains of 2.0 nm to 2.5 nm. The corresponding singlet diffusivity of C_{60} is $D = 4.2 \times 10^{-3} \text{ cm}^2/\text{sec}$ and we calculate a singlet exciton diffusion length of $L_D = 10 \pm 4 \text{ nm}$ in C_{60} using the Monte Carlo simulation and the C_{60} singlet lifetime (150 ps).²⁹ Peumans *et al.* reported $L_D = 40 \pm 5 \text{ nm}$ for C_{60} ,³⁰ reflecting the contribution of triplet excitons to the photocurrent under CW illumination.

The TRTS and TA signals persist past 1 ns, requiring CW spectroscopy to study recombination dynamics. Fig. 3 shows the PA and absorption spectra of samples with (a) 10 nm and (b) 2 nm thick layers. For 10 nm layers, there are one strong and two weak PA bands and GSB of $ZnPc$. PA band A_1 at 1.1 eV originates from C_{60} anions.³² The energies and relative intensities of PA bands C_1 at 1.45 eV and C_2 at 2.30 eV match the absorption of oxidized $ZnPc$ ^{33,34} and are assigned to $ZnPc$ cations. The GSB is more structured than the absorption of $ZnPc$ as the excited states inhabit a narrower energy range of sites. As the layer thickness is reduced, a new band emerges (X_1) at 1.66 eV and C_2 broadens. The PA spectra of the blend [Fig. 3(b)] is similar, but only half as strong. The PA spectrum of a neat film of C_{60} (not shown) was consistent with previous work.³¹ The strongest feature is an electroabsorption maxima at 2.2 eV ($\Delta T/T = 5 \times 10^{-5}$). No significant PA was observed from a neat $ZnPc$ film ($\Delta T/T < 10^{-6}$).

There are striking differences in recombination dynamics between the two films. The insets to Fig. 3 show (a) the dependence of the C_2 and GSB on laser power and (b) decay dynamics of C_2 following excitation. Both PA

and GSB increase with the square root of the laser power for the 10 nm layered sample, indicating bimolecular recombination, whereas the signals increase linearly with laser power for 2 nm layered sample as well as the blend. The decay of PA and GSB of the 10 nm layered sample slows with time, consistent with bimolecular recombination ($dn/dt \propto n^2$). The reciprocal recombination rate is $67 \pm 3 \mu\text{s}$. The decays of the C_2 and X_1 of the 2 nm layered sample are correlated with one another and can be fit to exponential decay ($\tau = 144 \pm 2 \mu\text{s}$). The GSB decay is more complicated, consisting of a strong, fast component correlated with the PA decays ($\tau = 0.2 \text{ ms}$) and a weak long-lived component ($\tau = 1.8 \text{ ms}$).

These results demonstrate the sensitivity of photocarriers to the heterojunction. Monomolecular recombination for films with ultrathin layers and blends indicates the formation of a bound state. Changes in recombination dynamics are accompanied by the emergence of a new PA band. Neutral states of C_{60} or $ZnPc$ are precluded as no such PA is seen in neat films. The best explanation for a metastable state associated with charge transfer is a $C_{60}^-/ZnPc^+$ exciplex. Such charge transfer states play a crucial role in organic solar cells, as both the photocurrent density (J) and voltage (V) directly depend upon them. Nonradiative recombination is a significant loss factor, up to 0.3 V, and thus must be suppressed.^{35,36} Typical lifetimes for exciplex emission are of order 10^{-8} sec to 10^{-7} sec ,^{36,37} whereas lifetimes in the range 10^{-6} sec to 10^{-4} sec are needed to obtain gain a good agreement between the measured $J - V$ of cells and models assuming geminate recombination.³⁸ Many open questions remain concerning recombination mechanisms in organic bulk heterojunctions. In light of such ongoing interest, our observation of such a long-lived exciplex at a molecular heterojunction is significant.

To conclude, transient THz and absorption spectroscopy shows that autoionization of C_{60} forms a short-lived charge transfer state. Decay of the TRTS signal following charge transfer reflects a decrease in carrier mobility over the first 20 ps and subsequently results from recombination. Singlet exciton migration within the C_{60} layer is manifested by a rise in GSB of $ZnPc$ absorption, permitting us to determine the diffusivity of singlet excitons in C_{60} . Finally, CW spectroscopy reveals a metastable $C_{60}^-/ZnPc^+$ exciplex. This work was supported by the Office of Naval Research and by NIST. P.C. thanks the National Research Council for administering the postdoctoral fellowship program at NRL.

* Current address Chemistry Department, Middle East Technical University, Ankara, Turkey.

¹ C. W. Tang, S. A. VanSlyke, and C. H. Chen, *Appl. Phys. Lett.* **55**, 3610 (1989).

² A. J. Heeger, *Chem. Soc. Rev.* **39**, 2354 (2010).

³ M. Riede *et al.*, *Adv. Func. Mater.* **21**, 3019 (2011).

⁴ G. Li, V. Shrotriya, J. S. Huang, Y. Yao, T. Moriarty,

K. Emery and Y. Yang, *Nature Mater.* **4**, 864 (2005).

⁵ Z. R. Hong, B. Maennig, R. Lessmann, M. Pfeiffer, and K. Leo, *Appl. Phys. Lett.* **90**, 203505 (2007).

⁶ I. Kim, H. M. Haverinen, J. A. Li, and G. E. Jabbour, *Appl. Phys. Lett.* **97**, 203301 (2010).

⁷ S. Pfuetzner *et al.*, *Org. Elec.* **12**, 435 (2011)

⁸ G. Ruani *et al.*, *Synth. Met.* **103**, 2392 (1999).

- ⁹ G. J. Dutton, W. Jin, J. E. Reutt-Robey and S. W. Robey, Phys. Rev. B **82**, 073407 (2010).
- ¹⁰ A. F. Bartelt, C. Strothkmper, W. Schindler, K. Fotiropoulos, and R. Eichberger, Appl. Phys. Lett. **99**, 143304 (2011).
- ¹¹ R. Ulbricht, E. Hendry, J. Shan, T. F. Heinz and M. Bonn, Rev. Mod. Phys. **83**, 543 (2011).
- ¹² E. Hendry, J. M. Schins, L. P. Candeias, L. D. A. Siebbeles and M. Bonn, Phys. Rev. Lett. **92**, 196601 (2004).
- ¹³ H. Nemeć, H. K. Nienhuys, E. Perzon, F. Zhang, O. Inganäs, P. Kuzel, and V. Sundström, Phys. Rev. B **79**, 245326 (2009).
- ¹⁴ X. Ai, M. C. Beard, K. P. Knutsen, S. E. Shaheen, G. Rumbles and R. J. Ellingson, J. Phys. Chem. B **110**, 25462 (2006).
- ¹⁵ F. A. Hegmann, R. R. Tykwiński, K. P. H. Lui, J. E. Bullock and J. E. Anthony, Phys. Rev. Lett. **89**, 227403 (2002).
- ¹⁶ P. Parkinson, J. Lloyd-Hughes, M. B. Johnston and L. M. Herz, Phys. Rev. B **78**, 115321 (2008).
- ¹⁷ P. D. Cunningham and L. M. Hayden, J. Phys. Chem. C **112**, 7928 (2008).
- ¹⁸ P. A. Lane *et al.*, SPIE Proc. **7416**, 74161Z (2009).
- ¹⁹ H.-K. Nienhuys and V. Sundström, Phys. Rev. B **71**, 235110 (2005).
- ²⁰ O. Esenturk, J. S. Melinger, P. A. Lane and E. J. Heilweil, J. Phys. Chem. C **113**, 18842 (2009).
- ²¹ N. Geactinov and M. Pope, J. Chem. Phys. **47**, 1194 (1967).
- ²² M. Wojcik and M. Tachiya, J. Chem. Phys. **130**, 104107 (2009).
- ²³ E. Frankevich, Y. Maruyama, and H. Ogata, Chem. Phys. Lett. **241**, 39 (1993).
- ²⁴ D. Sarkar and N. J. Halas, Solid State Comm. **90**, 261 (1994).
- ²⁵ C. H. Lee, G. Yu, D. Moses, V. I. Srđanov, X. Wei, and Z. V. Vardeny, Phys. Rev. B **48**, 8506 (1993).
- ²⁶ T. J. Savenije *et al.* J. Phys. Chem. Lett. **2**, 1368 (2011).
- ²⁷ See Supplemental Material
- ²⁸ N. E. Coates, D. Moses and A. J. Heeger, Appl. Phys. Lett. **98**, 102103 (2011).
- ²⁹ B. C. Hess, E. A. Forgy, S. Frolov, D. D. Dick, and Z. V. Vardeny, Phys. Rev. B **50**, 4871 (1994).
- ³⁰ P. Peumans, A. Yakimov, and S. R. Forrest, J. Appl. Phys. **93**, 3693 (2003).
- ³¹ D. Dick *et al.*, Phys. Rev. Lett **73**, 2760 (1994).
- ³² K. Lee, R. A. J. Janssen, N. S. Sariciftci, and A. J. Heeger, Phys. Rev. B **49** 5781 (1994).
- ³³ J. M. Green and L. R. Faulkner, J. Am. Chem Soc. **105**, 2950 (1983).
- ³⁴ J. Mack and M. J. Stillman, Coord. Chem. Rev. **219-221**, 993 (2001).
- ³⁵ K. Vandewal, K. Tvingstedt, A. Gadisa, O. Inganäs, J. V. Manca, Nat. Mater. **904**, 8 (2009).
- ³⁶ N. C. Giebink, B. E. Lassiter, G. P. Wiederrecht, M. R. Wasielewski, and S. R. Forrest, Phys. Rev. B **82**, 155306 (2010).
- ³⁷ D. Veldman *et al.*, J. Am. Chem. Soc. **130**, 7721 (2008).
- ³⁸ C. Deibel, T. Strobel and V. Dyakonov, Adv. Mater. **22**, 4097 (2010).

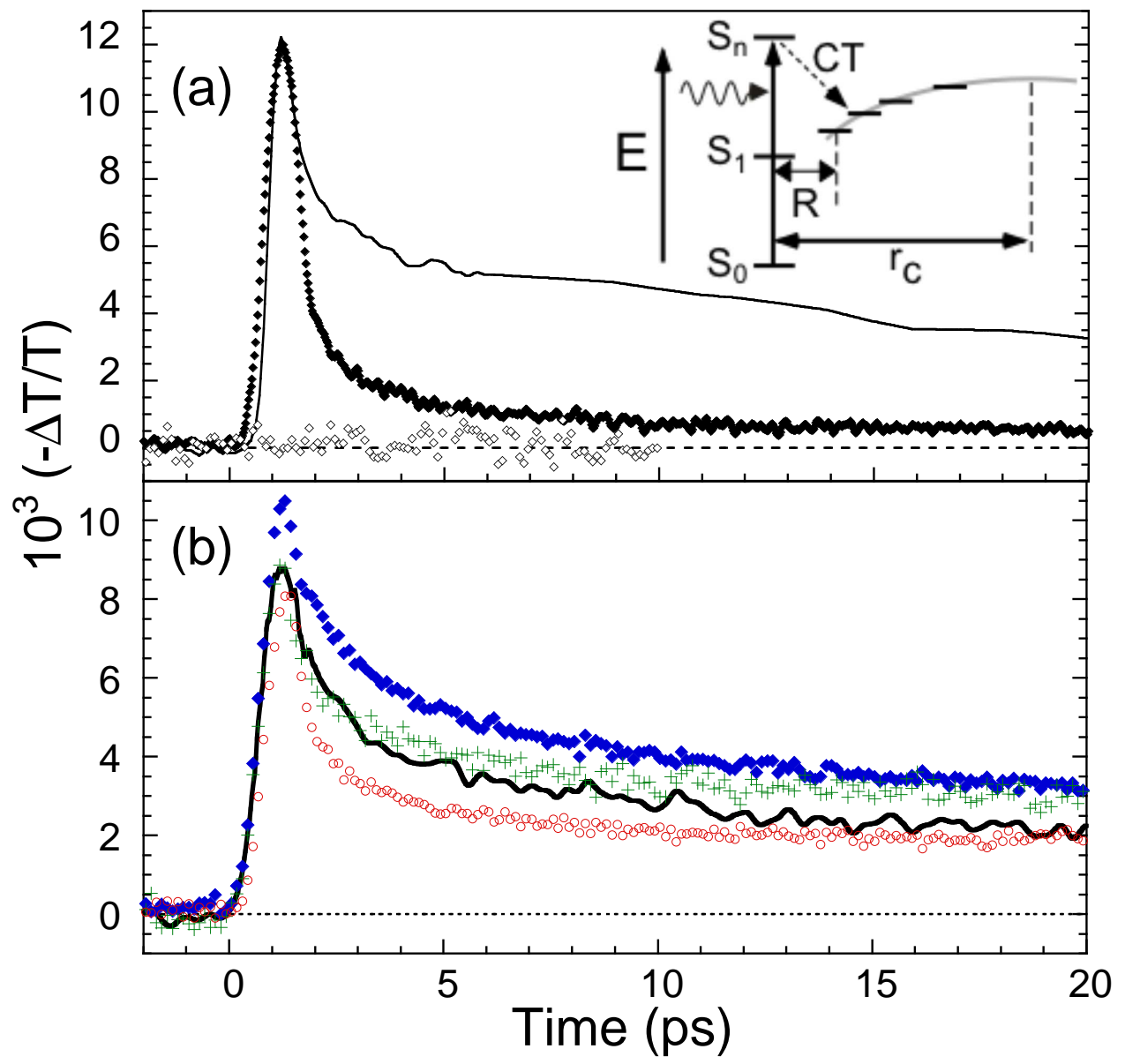


Figure 1 LH13276 04JAN12

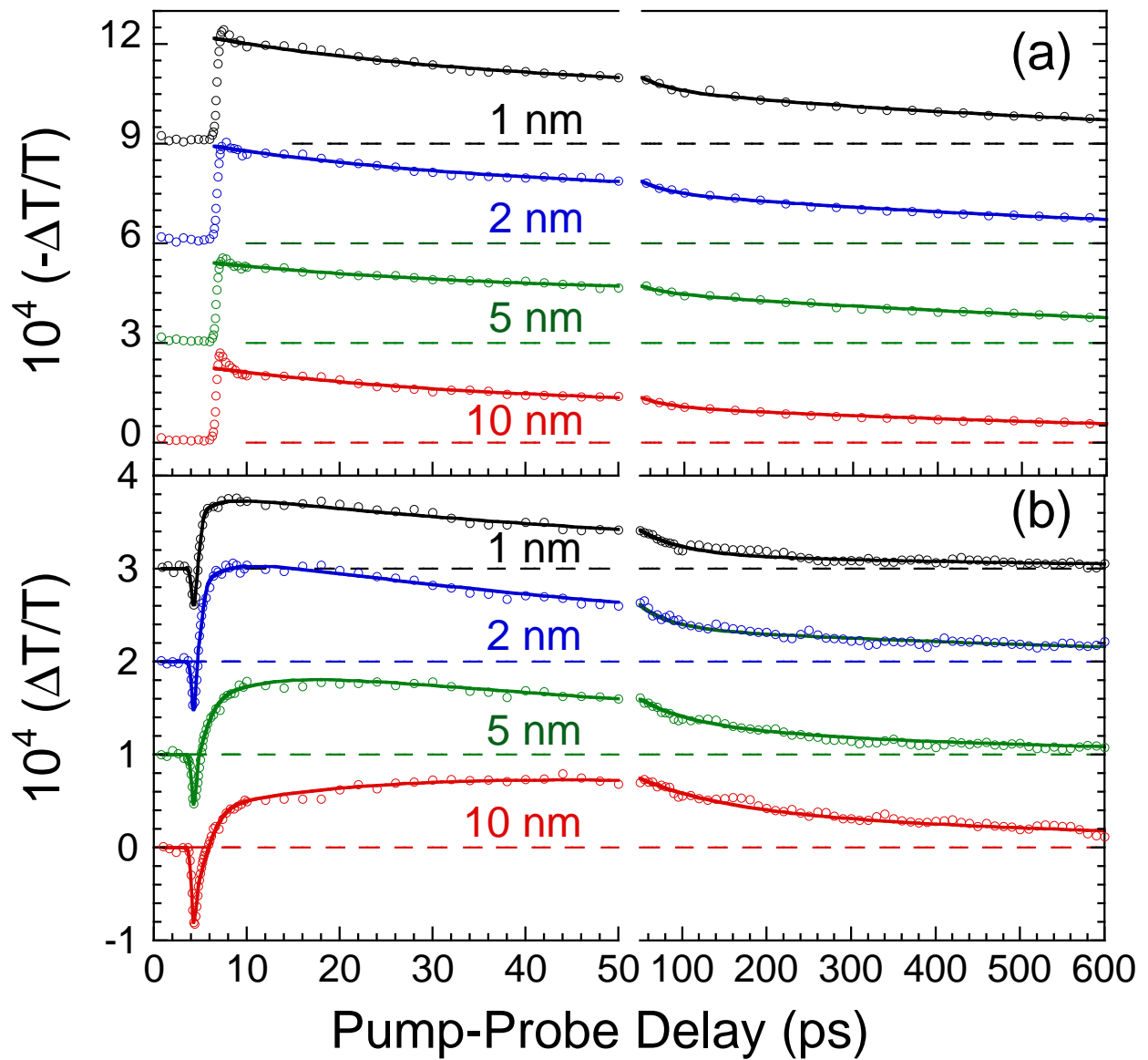


Figure 2

LH13276 04JAN12

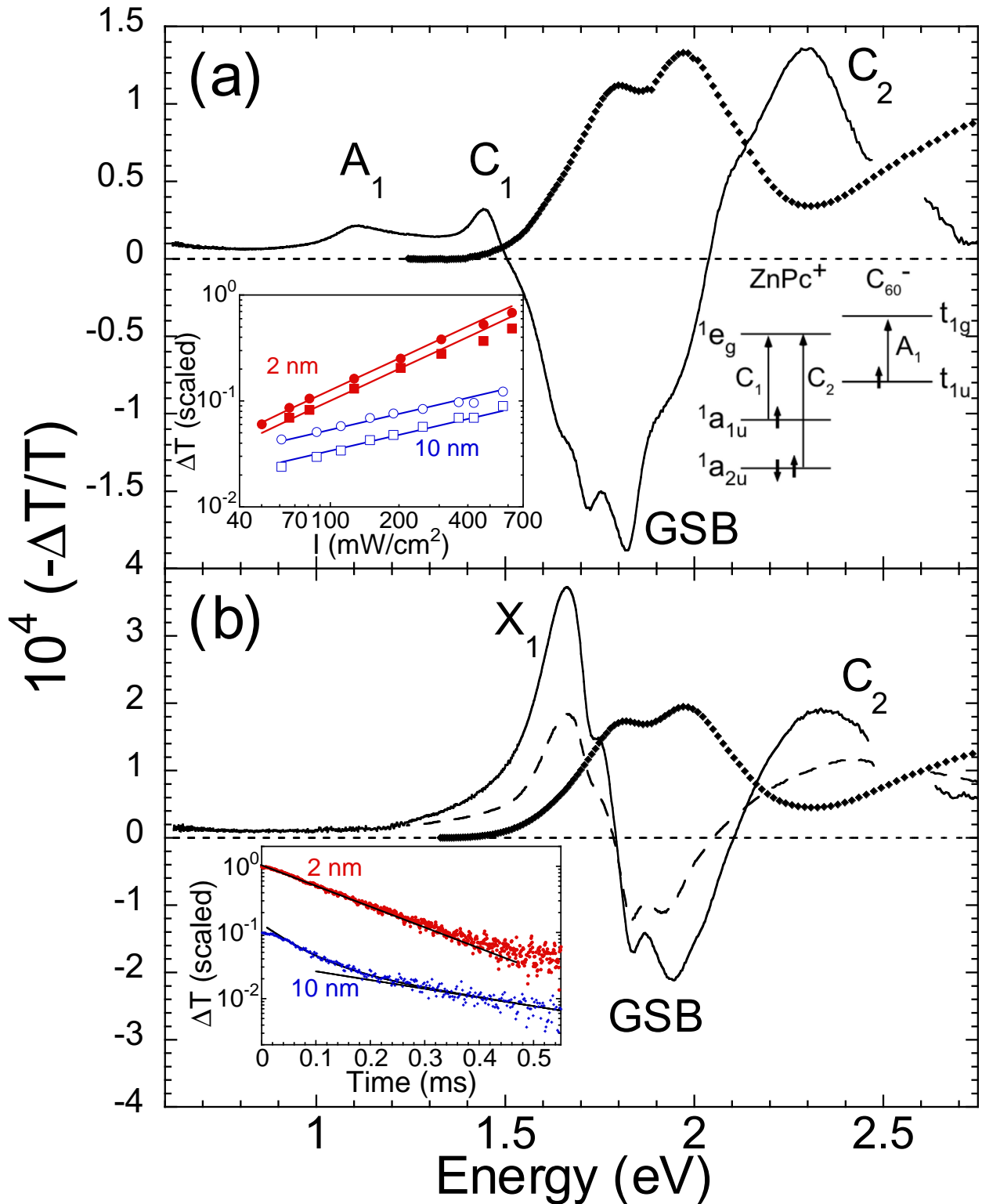


Figure 3

LH13276 04JAN12